MATLAB Functions for Mie Scattering and Absorption
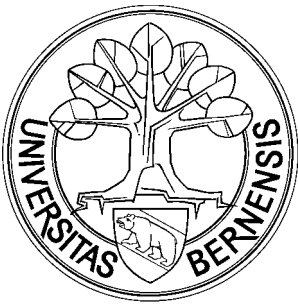
Christian Mätzler

Institut für Angewandte Physik

Mikrowellenabteilung

Sidlerstrasse 5
3012 Bern
Schweiz

Tel.   : +41 31 631 89 11
Fax.   : +41 31 631 37 65
E-mail : matzler@iap.unibe.ch

MATLAB Functions for Mie Scattering and Absorption

Christian Mätzler, Institute of Applied Physics, University of Bern, June 2002[1]

List of Contents

Abstract

A set of Mie functions has been developed in MATLAB to compute the four Mie coefficients a_n, b_n, c_n and d_n, efficiencies of extinction, scattering, backscattering and absorption, the asymmetry parameter, and the two angular scattering functions S_1 and S_2. In addition to the scattered field, also the absolute-square of the internal field is computed and used to get the absorption efficiency in a way independent from the scattered field. This allows to test the computational accuracy.

This first version of MATLAB Mie Functions is limited to homogeneous dielectric spheres without change in the magnetic permeability between the inside and outside of the particle. Required input parameters are the complex refractive index, $m = m' + im''$, of the sphere (relative to the ambient medium) and the size parameter, $x = ka$, where a is the sphere radius and k the wave number in the ambient medium.

---

[1] Equation on p. 16 corrected, April 2006

1 Introduction

This report is a description of Mie-Scattering and Mie-Absorption programs written in the numeric computation and visualisation software, MATLAB (Math Works, 1992), for the improvement of radiative-transfer codes, especially to account for rain and hail in the microwave range and for aerosols and clouds in the submillimeter, infrared and visible range. Excellent descriptions of Mie Scattering were given by van de Hulst (1957) and by Bohren and Huffman (1983). The present programs are related to the formalism of Bohren and Huffman (1983). In addition an extension (Section 2.5) is given to describe the radial dependence of the internal electric field of the scattering sphere and the absorption resulting from this field. Except for Section 2.5, equation numbers refer to those in Bohren and Huffman (1983), in short BH, or in case of missing equation numbers, page numbers are given. For a description of computational problems in the Mie calculations, see the notes on p. 126-129 and in Appendix A of BH.

2 Formulas for a homogeneous sphere

2.1 Mie coefficients and Bessel functions

MATLAB function: Mie_abcd
The key parameters for Mie calculations are the Mie coefficients a_n and b_n to compute the amplitudes of the scattered field, and c_n and d_n for the internal field, respectively. The computation of these parameters has been the most challenging part in Mie computations due to the involvement of spherical Bessel functions up to high order. With MATLAB's built-in double-precision Bessel functions, the computation of the Mie coefficients has so far worked well up to size parameters exceeding 10'000; the coefficients are given in BH on p.100:

$$a_n = \frac{m^2 j_n(mx)[xj_n(x)]' - \mu_1 j_n(x)[mxj_n(mx)]'}{m^2 j_n(mx)[xh_n^{(1)}(x)]' - \mu_1 h_n^{(1)}(x)[mxj_n(mx)]'}$$

$$b_n = \frac{\mu_1 j_n(mx)[xj_n(x)]' - j_n(x)[mxj_n(mx)]'}{\mu_1 j_n(mx)[xh_n^{(1)}(x)]' - h_n^{(1)}(x)[mxj_n(mx)]'}$$

(4.53)

$$c_n = \frac{\mu_1 j_n(x)[xh_n^{(1)}(x)]' - \mu_1 h_n^{(1)}(x)[xj_n(x)]'}{\mu_1 j_n(mx)[xh_n^{(1)}(x)]' - h_n^{(1)}(x)[mxj_n(mx)]'}$$

$$d_n = \frac{\mu_1 m j_n(x)[xh_n^{(1)}(x)]' - \mu_1 m h_n^{(1)}(x)[xj_n(x)]'}{m^2 j_n(mx)[xh_n^{(1)}(x)]' - \mu_1 h_n^{(1)}(x)[mxj_n(mx)]'}$$

(4.52)

where m is the refractive index of the sphere relative to the ambient medium, $x=ka$ is the size parameter, a the radius of the sphere and $k = 2\pi/\lambda$ is the wave number and λ the wavelength in the ambient medium. In deviation from BH, μ_1 is the ratio of the magnetic permeability of the sphere to the magnetic permeability of the ambient medium (corresponding to μ_1/μ in BH). The functions $j_n(z)$ and $h_n^{(1)}(z) = j_n(z) + iy_n(z)$ are spherical Bessel functions of order n (n= 1, 2,..) and of the given arguments, $z= x$ or mx, respectively, and primes mean derivatives with respect to the argument. The derivatives follow from the spherical Bessel functions themselves, namely

$$[zj_n(z)]' = zj_{n-1}(z) - nj_n(z); \quad [zh_n^{(1)}(z)]' = zh_{n-1}^{(1)}(z) - nh_n^{(1)}(z) \qquad (p.127)$$

For completeness, the following relationships between Bessel and spherical Bessel functions are given:

$$j_n(z) = \sqrt{\frac{\pi}{2z}} J_{n+0.5}(z) \tag{4.9}$$

$$y_n(z) = \sqrt{\frac{\pi}{2z}} Y_{n+0.5}(z) \tag{4.10}$$

Here, J_v and Y_v are Bessel functions of the first and second kind. For $n=0$ and 1 the spherical Bessel functions are given (BH, p. 87) by

$$j_0(z) = \sin z / z; \; j_1(z) = \sin z / z^2 - \cos z / z$$
$$y_0(z) = -\cos z / z; \; y_1(z) = -\cos z / z^2 - \sin z / z$$

and the recurrence formula

$$f_{n-1}(z) + f_{n+1}(z) = \frac{2n+1}{z} f_n(z) \tag{4.11}$$

where f_n is any of the functions j_n and y_n. Taylor-series expansions for small arguments of j_n and y_n are given on p. 130 of BH. The spherical Hankel functions are linear combinations of j_n and y_n. Here, the first type is required

$$h_n^{(1)}(z) = j_n(z) + iy_n(z) \tag{4.13}$$

The following related functions are also used in Mie theory (although we try to avoid them here):

$$\psi_n(z) = zj_n(z); \; \chi_n(z) = -zy_n(z); \; \xi_n(z) = zh_n^{(1)}(z) \tag{p.101, 183}$$

Often $\mu_1=1$; then, (4.52-4.53) simplify to

$$a_n = \frac{m^2 j_n(mx)[xj_n(x)]' - j_n(x)[mxj_n(mx)]'}{m^2 j_n(mx)[xh_n^{(1)}(x)]' - h_n^{(1)}(x)[mxj_n(mx)]'} ;$$

$$b_n = \frac{j_n(mx)[xj_n(x)]' - j_n(x)[mxj_n(mx)]'}{j_n(mx)[xh_n^{(1)}(x)]' - h_n^{(1)}(x)[mxj_n(mx)]'}$$

$$c_n = \frac{j_n(x)[xh_n^{(1)}(x)]' - h_n^{(1)}(x)[xj_n(x)]'}{j_n(mx)[xh_n^{(1)}(x)]' - h_n^{(1)}(x)[mxj_n(mx)]'} ;$$

$$d_n = \frac{mj_n(x)[xh_n^{(1)}(x)]' - mh_n^{(1)}(x)[xj_n(x)]'}{m^2 j_n(mx)[xh_n^{(1)}(x)]' - h_n^{(1)}(x)[mxj_n(mx)]'}$$

The parameters used in radiative transfer depend on a_n and b_n, but not on c_n and d_n. The latter coefficients are needed when the electric field inside the sphere is of interest, e.g. to test the field penetration in the sphere, to study the distribution of heat sources or to compute absorption. The absorption efficiency Q_{abs}, however, can also be computed from the scattered radiation, Equations (3.25), (4.61-62) to be shown below.

2.2 Mie efficiencies and cross sections

MATLAB functions: Mie, Mie_xscan

The efficiencies Q_i for the interaction of radiation with a scattering sphere of radius a are cross sections σ_i (called C_i in BH) normalised to the particle cross section, πa^2, where i stands for extinction ($i=ext$), absorption ($i=abs$), scattering ($i=sca$), back-scattering ($i=b$), and radiation pressure ($i=pr$), thus

$$Q_i = \frac{\sigma_i}{\pi\, a^2}$$

Energy conservation requires that

$$Q_{ext} = Q_{sca} + Q_{abs}, \text{ or } \sigma_{ext} = \sigma_{sca} + \sigma_{abs} \tag{3.25}$$

The scattering efficiency Q_{sca} follows from the integration of the scattered power over all directions, and the extinction efficiency Q_{ext} follows from the Extinction Theorem (Ishimaru, 1978, p. 14, van de Hulst, 1957, p. 31), also called Forward-Scattering Theorem, leading to:

$$Q_{sca} = \frac{2}{x^2} \sum_{n=1}^{\infty} (2n+1)(|a_n|^2 + |b_n|^2) \tag{4.61}$$

$$Q_{ext} = \frac{2}{x^2} \sum_{n=1}^{\infty} (2n+1)\,\mathrm{Re}(a_n + b_n) \tag{4.62}$$

and Q_{abs} follows from (3.25). All infinite series can be truncated after n_{max} terms. For this number Bohren and Huffman (1983) proposed the value

$$n_{max} = x + 4x^{1/3} + 2 \tag{p.477}$$

and this value is used here as well.

Furthermore, the asymmetry parameter $g=\langle\cos\theta\rangle$ indicates the average cosine of the scattering angle θ with respect to power; it is used in Two-Stream Models (Meador and Weaver, 1980), and it is related to the efficiency Q_{pr} of radiation pressure:

$$Q_{pr} = Q_{ext} - Q_{sca}\langle\cos\theta\rangle \tag{p.120}$$

$$Q_{sca}\langle\cos\theta\rangle = \frac{4}{x^2}\left\{ \sum_{n=1}^{\infty} \frac{n(n+2)}{n+1}\mathrm{Re}(a_n a_{n+1}^* + b_n b_{n+1}^*) + \sum_{n=1}^{\infty} \frac{2n+1}{n(n+1)}\mathrm{Re}(a_n b_n^*) \right\}$$

Finally, the backscattering efficiency Q_b, applicable to monostatic radar, is given by

$$Q_b = \frac{1}{x^2}\left| \sum_{n=1}^{\infty} (2n+1)(-1)^n (a_n - b_n) \right|^2 \tag{p.122}$$

2.3 The scattered far field

MATLAB functions: Mie_S12, Mie_pt, Mie_tetascan

If the detailed shape of the angular scattering pattern is required, e.g. to get the phase matrix or phase function for radiative-transfer calculations (Chandrasekhar, 1960), the scattering functions S_1 and S_2 are required. These functions describe the scattered field $\mathbf{E_s}$. The scattered far field in spherical coordinates ($E_{s\theta}$, $E_{s\phi}$) for a unit-amplitude incident field (where the time variation exp(-iωt) has been omitted) is given by

$$E_{s\theta} = \frac{e^{ikr}}{-ikr}\cos\phi \cdot S_2(\cos\theta)$$

$$E_{s\phi} = \frac{e^{ikr}}{ikr}\sin\phi \cdot S_1(\cos\theta)$$

with the scattering amplitudes S_1 and S_2

$$S_1(\cos\theta) = \sum_{n=1}^{\infty} \frac{2n+1}{n(n+1)}(a_n\pi_n + b_n\tau_n);$$

$$(4.74)$$

$$S_2(\cos\theta) = \sum_{n=1}^{\infty} \frac{2n+1}{n(n+1)}(a_n\tau_n + b_n\pi_n)$$

$E_{s\theta}$ is the scattered far-field component in the scattering plane, defined by the incident and scattered directions, and $E_{s\phi}$ is the orthogonal component. The angle ϕ is the angle between the incident electric field and the scattering plane. The functions $\pi_n(\cos\theta)$ and $\tau_n(\cos\theta)$ describe the angular scattering patterns of the spherical harmonics used to describe S_1 and S_2 and follow from the recurrence relations

$$\pi_n = \frac{2n-1}{n-1}\cos\theta \cdot \pi_{n-1} - \frac{n}{n-1}\pi_{n-2}; \quad \tau_n = n\cos\theta \cdot \pi_n - (n+1)\pi_{n-1} \quad (4.47)$$

starting with (Deirmendjian, 1969, p. 15)

$$\pi_0 = 0; \pi_1 = 1; \pi_2 = 3\cos\theta; \tau_0 = 0; \tau_1 = \cos\theta; \tau_2 = 3\cos(2\theta)$$

2.4 The internal field

MATLAB function: presently, no direct function, but see Mie_Esquare
The internal field $\mathbf{E}_1$ for an incident field with unit amplitude is given by

$$\mathbf{E}_1 = \sum_{n=1}^{\infty} \frac{2n+1)}{n(n+1)}\left(c_n\mathbf{M}_{o1n}^{(1)} - d_n\mathbf{N}_{e1n}^{(1)}\right)$$

$$(4.40)$$

where the vector-wave harmonic fields are given in spherical (r,θ,ϕ) coordinates by

$$\mathbf{M}_{o1n}^{(1)} = \begin{pmatrix} 0 \\ \cos\phi \cdot \pi_n(\cos\theta)j_n(rmx) \\ -\sin\phi \cdot \tau_n(\cos\theta)j_n(rmx) \end{pmatrix}$$

$$\mathbf{N}_{e1n}^{(1)} = \begin{pmatrix} n(n+1)\cos\phi \cdot \sin\theta \cdot \pi_n(\cos\theta)\dfrac{j_n(rmx)}{rmx} \\ \cos\phi \cdot \tau_n(\cos\theta)\dfrac{[rmxj_n(rmx)]'}{rmx} \\ -\sin\phi \cdot \pi_n(\cos\theta)\dfrac{[rmxj_n(rmx)]'}{rmx} \end{pmatrix}$$

$$(4.50)$$

and the coordinate system is defined as for the scattered field. The vector-wave functions $\mathbf{N}$ and $\mathbf{M}$ are orthogonal with respect to integration over directions. Furthermore for different values of n, the $\mathbf{N}$ functions are orthogonal, too, and the same is true for the $\mathbf{M}$ functions.

2.5 Computation of Q_abs, based on the internal field

MATLAB functions: Mie_Esquare, Mie_abs

The absorption cross section of a particle with dielectric (i.e. Ohmic) losses is given by (Ishimaru, 1978, p. 17)

$$\sigma_{abs} = k\varepsilon'' \int_V |\mathbf{E}_1|^2 \, dV \qquad (1)$$

where ε" is the imaginary part of the relative dielectric constant of the particle (here with respect to the ambient medium). Thanks to the orthogonality of the spherical vector-wave functions this integral becomes in spherical coordinates

$$\sigma_{abs} = k\varepsilon''\pi \sum_{n=1}^{\infty} \int_{-1}^{+1} d(\cos\theta) \int_0^a r^2 dr \left(|c_n|^2 (m_\theta + m_\phi) + |d_n|^2 (n_r + n_\theta + n_\phi) \right) \qquad (2)$$

and the integration over azimuth φ has already been performed, leading to the factor π. The functions in the integrand are absolute-square values of the series terms of the components of the vector-waves (4.50)

$$m_\theta = g_n \pi_n^2(\cos\theta) \cdot |j_n(z)|^2$$

$$m_\phi = g_n \tau_n^2(\cos\theta) \cdot |j_n(z)|^2$$

$$n_r = g_n \sin^2\theta \cdot \pi_n^2(\cos\theta) \left| \frac{j_n(z)}{z} \right|^2 \qquad (3)$$

$$n_\theta = g_n \tau_n^2(\cos\theta) \left| \frac{(zj_n(z))'}{z} \right|^2$$

$$n_\phi = g_n \pi_n^2(\cos\theta) \left| \frac{(zj_n(z))'}{z} \right|^2$$

Here $z = mrk$, and g_n stands for

$$g_n = \left(\frac{2n+1}{n(n+1)} \right)^2 \qquad (4)$$

For the integrals over cosθ, analytic solutions can be obtained. First, from BH we find

$$\int_{-1}^{1} \left(\pi_n^2(\cos\theta) + \tau_n^2(\cos\theta) \right) d(\cos\theta) = \frac{2n^2(n+1)^2}{2n+1} \qquad (p.103)$$

and second, from (4.46) in BH and Equation 8.14.13 of Abramowitz and Stegun (1965), we get

$$\int_{-1}^{1} \left(\sin^2\theta \cdot \pi_n^2(\cos\theta) \right) d(\cos\theta) = \int_{-1}^{1} \left(P_n^1(\cos\theta) \right)^2 d(\cos\theta) = \frac{2(n+1)}{2n+1} \qquad (5)$$

leading to the two parts (6) and (7) of the angular integral in (2)

$$m_n = \int_{-1}^{1} \left(m_\theta + m_\phi \right) d(\cos\theta) = 2(2n+1)|j_n(z)|^2 \qquad (6)$$

$$n_n = \int_{-1}^{1}(n_r + n_\theta + n_\phi)d(\cos\theta) = 2n(2n+1)\left\{(n+1)\left|\frac{j_n(z)}{z}\right|^2 + \left|\frac{(zj_n(z))'}{z}\right|^2\right\} \qquad (7)$$

Now, the absorption cross section follows from integration over the radial distance r inside the sphere up to the sphere radius a:

$$\sigma_{abs} = k\varepsilon''\pi\sum_{n=1}^{\infty}\int_0^a\left(m_n|c_n|^2 + n_n|d_n|^2\right)r^2 dr \qquad (8)$$

The integrand contains the radial dependence of the absolute-square electric field $\langle|\mathbf{E}|^2\rangle$ averaged over spherical shells (all θ and ϕ, constant r):

$$\langle|\mathbf{E}|^2\rangle = \frac{1}{4}\sum_{n=1}^{\infty}\left(m_n|c_n|^2 + n_n|d_n|^2\right) \qquad (9)$$

and in terms of this quantity, the absorption efficiency becomes

$$Q_{abs} = \frac{4\varepsilon''}{x^2}\int_0^x\langle|\mathbf{E}|^2\rangle x'^2\,dx' \qquad (10)$$

where $x'=rk=z/m$. Note that (9) is dimensionless because of the unit-amplitude incident field; In case of Rayleigh scattering ($x\ll1$) the internal field is constant, and the corresponding squared-field ratio (9) is given by

$$\frac{9}{|m^2 + 2|^2} \qquad (11)$$

This quantity can be used to test the accuracy of the function, Mie_Esquare, for small size parameters. In addition, Equation (10) can be used to test the accuracy of the computation of Q_{abs} from the difference, $Q_{ext} - Q_{sca}$ (4.61-62). Finally, it should be remembered that all infinite series can be terminated after n_{max} terms.

3 The MATLAB Programs

3.1 Comments

3.1.1 Restrictions
1. The present restrictions are situations with $\mu_1=1$; this means that the permittivity of the sphere relative to the ambient medium is given by $\varepsilon=m^2$.
2. There is a maximum x value for stable and correct computation of Mie scattering. For a small or moderate imaginary refractive index m'', the maximum size parameter ranges somewhere between 10^4 and 10^5, however, for $m''\gg1$, the maximum size parameter is strongly diminished.

3.1.2 Computation of Bessel Functions
The ordinary Bessel Functions $J_\nu(z)$ and $Y_\nu(z)$ are standard functions in MATLAB. The spherical Bessel Functions used here follow from (4.9-10) of BH.

3.1.3 Computation of angular functions
The angular functions, π_n and τ_n, are computed from the recurrence relations (4.47) of BH with the initial functions given for $n=1$ and 2.

3.1.4 Optimisation strategy

The programs were optimised rather with respect to computation speed than memory space; all required function values are computed only once and then stored for further use in vectors of dimension n_{max}.

3.2 The Function Mie_abcd

The following text lists the basic program to compute the **Mie Coefficients** a_n, b_n, c_n, d_n and to produce a matrix of n_{max} column vectors $[a_n; b_n; c_n; d_n]$:

```
function result = Mie_abcd(m, x)

% Computes a matrix of Mie coefficients, a_n, b_n, c_n, d_n,
% of orders n=1 to nmax, complex refractive index m=m'+im",
% and size parameter x=k0*a, where k0= wave number
% in the ambient medium, a=sphere radius;
% p. 100, 477 in Bohren and Huffman (1983) BEWI:TDD122
% C. Mätzler, June 2002

nmax=round(2+x+4*x^(1/3));
n=(1:nmax); nu = (n+0.5); z=m.*x; m2=m.*m;
sqx= sqrt(0.5*pi./x); sqz= sqrt(0.5*pi./z);
bx = besselj(nu, x).*sqx;
bz = besselj(nu, z).*sqz;
yx = bessely(nu, x).*sqx;
hx = bx+i*yx;
b1x=[sin(x)/x, bx(1:nmax-1)];
b1z=[sin(z)/z, bz(1:nmax-1)];
y1x=[-cos(x)/x, yx(1:nmax-1)];
h1x= b1x+i*y1x;
ax = x.*b1x-n.*bx;
az = z.*b1z-n.*bz;
ahx= x.*h1x-n.*hx;
an = (m2.*bz.*ax-bx.*az)./(m2.*bz.*ahx-hx.*az);
bn = (bz.*ax-bx.*az)./(bz.*ahx-hx.*az);
cn = (bx.*ahx-hx.*ax)./(bz.*ahx-hx.*az);
dn = m.*(bx.*ahx-hx.*ax)./(m2.*bz.*ahx-hx.*az);
result=[an; bn; cn; dn];
```

3.3 The Function Mie

The following text lists the Program to compute the **Mie Efficiencies**:

```
function result = Mie(m, x)

% Computation of Mie Efficiencies for given
% complex refractive-index ratio m=m'+im"
% and size parameter x=k0*a, where k0= wave number in ambient
% medium, a=sphere radius, using complex Mie Coefficients
% an and bn for n=1 to nmax,
% s. Bohren and Huffman (1983) BEWI:TDD122, p. 103,119-122,477.
% Result: m', m", x, efficiencies for extinction (qext),
% scattering (qsca), absorption (qabs), backscattering (qb),
% asymmetry parameter (asy=<costeta>) and (qratio=qb/qsca).
```

```
% Uses the function "Mie_abcd" for an and bn, for n=1 to nmax.
% C. Mätzler, May 2002.

if x==0              % To avoid a singularity at x=0
    result=[real(m) imag(m) 0 0 0 0 0 0 1.5];
elseif x>0           % This is the normal situation
 nmax=round(2+x+4*x^(1/3));
    n1=nmax-1;
    n=(1:nmax);cn=2*n+1; c1n=n.*(n+2)./(n+1); c2n=cn./n./(n+1);
    x2=x*x;
    f=mie_abcd(m,x);
    anp=(real(f(1,:))); anpp=(imag(f(1,:)));
    bnp=(real(f(2,:))); bnpp=(imag(f(2,:)));
    g1(1:4,nmax)=[0; 0; 0; 0]; % displaced numbers used for
    g1(1,1:n1)=anp(2:nmax);    % asymmetry parameter, p. 120
    g1(2,1:n1)=anpp(2:nmax);
    g1(3,1:n1)=bnp(2:nmax);
    g1(4,1:n1)=bnpp(2:nmax);
    dn=cn.*(anp+bnp);
    q=sum(dn);
    qext=2*q/x2;
    en=cn.*(anp.*anp+anpp.*anpp+bnp.*bnp+bnpp.*bnpp);
    q=sum(en);
    qsca=2*q/x2;
    qabs=qext-qsca;
    fn=(f(1,:)-f(2,:)).*cn;
    gn=(-1).^n;
    f(3,:)=fn.*gn;
    q=sum(f(3,:));
    qb=q*q'/x2;
    asy1=c1n.*(anp.*g1(1,:)+anpp.*g1(2,:)+bnp.*g1(3,:)+bnpp.*g1(4,:));
    asy2=c2n.*(anp.*bnp+anpp.*bnpp);
    asy=4/x2*sum(asy1+asy2)/qsca;
    qratio=qb/qsca;
    result=[real(m) imag(m) x qext qsca qabs qb asy qratio];
end;
```

3.4 The Function Mie_S12

The following text lists the program to compute the two **complex scattering amplitudes** S_1 and S_2:

```
function result = Mie_S12(m, x, u)

% Computation of Mie Scattering functions S1 and S2
% for complex refractive index m=m'+im",
% size parameter x=k0*a, and u=cos(scattering angle),
% where k0=vacuum wave number, a=sphere radius;
% s. p. 111-114, Bohren and Huffman (1983) BEWI:TDD122
% C. Mätzler, May 2002

nmax=round(2+x+4*x^(1/3));
abcd=Mie_abcd(m,x);
an=abcd(1,:);
```

```
bn=abcd(2,:);
pt=Mie_pt(u,nmax);
pin =pt(1,:);
tin=pt(2,:);
n=(1:nmax);
n2=(2*n+1)./(n.*(n+1));
pin=n2.*pin;
tin=n2.*tin;
S1=(an*pin'+bn*tin');
S2=(an*tin'+bn*pin');
result=[S1;S2];
```

3.5 The Function Mie_xscan

The following text lists the program to compute the a matrix of **Mie efficiencies** and to **plot** them as a function of x:

```
function result = Mie_xscan(m, nsteps, dx)

% Computation and plot of Mie Efficiencies for given
% complex refractive-index ratio m=m'+im"
% and range of size parameters x=k0*a,
% starting at x=0 with nsteps increments of dx
% a=sphere radius, using complex Mie coefficients an and bn
% according to Bohren and Huffman (1983) BEWI:TDD122
% result: m', m", x, efficiencies for extinction (qext),
% scattering (qsca), absorption (qabs), backscattering (qb),
% qratio=qb/qsca and asymmetry parameter (asy=<costeta>).
% C. Mätzler, May 2002.

nx=(1:nsteps)';
x=(nx-1)*dx;
for j = 1:nsteps
    a(j,:)=Mie(m,x(j));
end;
output_parameters='Real(m), Imag(m), x, Qext, Qsca, Qabs, Qb, <costeta>, Qb/Qsca'
m1=real(m);m2=imag(m);
plot(a(:,3),a(:,4:9))                    % plotting the results
legend('Qext','Qsca','Qabs','Qb','<costeta>','Qb/Qsca')
title(sprintf('Mie Efficiencies, m=%g+%gi',m1,m2))
xlabel('x')
result=a;
```

3.6 The Function Mie_tetascan

The following text lists the program to compute the a matrix of **Mie scattering intensities** $|S_1|^2$ and $|S_2|^2$ as a function of u=cosθ, and to display the result as a polar diagram of θ with $|S_1|^2$ in the upper half circle (0<θ<π) and $|S_2|^2$ in the lower half circle (π<θ<2π). Both functions are symmetric with respect to both half circles:

```
function result = Mie_tetascan(m, x, nsteps)
```

```
% Computation and plot of Mie Power Scattering function for given
% complex refractive-index ratio m=m'+im", size parameters x=k0*a,
% according to Bohren and Huffman (1983) BEWI:TDD122
% C. Mätzler, May 2002.

nsteps=nsteps;
m1=real(m); m2=imag(m);
nx=(1:nsteps); dteta=pi/(nsteps-1);
teta=(nx-1).*dteta;
   for j = 1:nsteps,
      u=cos(teta(j));
      a(:,j)=Mie_S12(m,x,u);
      SL(j)= real(a(1,j)'*a(1,j));
      SR(j)= real(a(2,j)'*a(2,j));
   end;
y=[teta teta+pi;SL SR(nsteps:-1:1)]';
polar(y(:,1),y(:,2))
title(sprintf('Mie angular scattering: m=%g+%gi, x=%g',m1,m2,x));
xlabel('Scattering Angle')
result=y;
```

3.7 The Function Mie_pt

The following text lists the program to compute a matrix of π_n and τ_n functions for n=1 to n_{max}:

```
function result=Mie_pt(u,nmax)

% pi_n and tau_n, -1 <= u= cosθ <= 1, n1 integer from 1 to nmax
% angular functions used in Mie Theory
% Bohren and Huffman (1983), p. 94 - 95

p(1)=1;
t(1)=u;
p(2)=3*u;
t(2)=3*cos(2*acos(u));
for n1=3:nmax,
   p1=(2*n1-1)./(n1-1).*p(n1-1).*u;
   p2=n1./(n1-1).*p(n1-2);
   p(n1)=p1-p2;
   t1=n1*u.*p(n1);
   t2=(n1+1).*p(n1-1);
   t(n1)=t1-t2;
end;
result=[p;t];
```

3.8 The Function Mie_Esquare

The following text lists the program to **compute** and **plot** the (θ, ϕ) averaged **absolute-square E-field** as a function of $x'=rk$ (for $r<0<a$):

```
function result = Mie_Esquare(m, x, nj)
```

```
% Computation of nj+1 equally spaced values within (0,x)
% of the mean-absolute-square internal
% electric field of a sphere of size parameter x,
% complex refractive index m=m'+im",
% where the averaging is done over teta and phi,
% with unit-amplitude incident field;
% Ref. Bohren and Huffman (1983) BEWI:TDD122,
% and my own notes on this topic;
% k0=2*pi./wavelength;
% x=k0.*radius;
% C. Mätzler, May 2002

nmax=round(2+x+4*x^(1/3));
n=(1:nmax);  nu =(n+0.5);
m1=real(m); m2=imag(m);
abcd=Mie_abcd(m,x);
cn=abcd(3,:);dn=abcd(4,:);
cn2=abs(cn).^2;
dn2=abs(dn).^2;
dx=x/nj;
for j=1:nj,
    xj=dx.*j;
    z=m.*xj;
    sqz= sqrt(0.5*pi./z);
    bz = besselj(nu, z).*sqz;       % This is jn(z)
    bz2=(abs(bz)).^2;
    b1z=[sin(z)/z, bz(1:nmax-1)];  % Note that sin(z)/z=j0(z)
    az = b1z-n.*bz./z;
    az2=(abs(az)).^2;
    z2=(abs(z)).^2;
    n1 =n.*(n+1);
    n2 =2.*(2.*n+1);
    mn=real(bz2.*n2);
    nn1=az2;
    nn2=bz2.*n1./z2;
    nn=n2.*real(nn1+nn2);
    en(j)=0.25*(cn2*mn'+dn2*nn');
end;
xxj=[0:dx:xj]; een=[en(1) en];
plot(xxj,een);
legend('Radial Dependence of (abs(E))^2')
title(sprintf('Squared Amplitude E Field in a Sphere, m=%g+%gi x=%g',m1,m2,x))
xlabel('r k')
result=een;
```

3.9 The Function Mie_abs

The following text lists the program to compute the **absorption efficiency**, based on Equation (9):

```
function result = Mie_abs(m, x)

% Computation of the Absorption Efficiency Qabs
% of a sphere of size parameter x,
```

% complex refractive index m=m'+im",
% based on nj internal radial electric field values
% to be computed with Mie_Esquare(nj,m,x)
% Ref. Bohren and Huffman (1983) BEWI:TDD122,
% and my own notes on this topic;
% k0=2*pi./wavelength;
% x=k0.*radius;
% C. Mätzler, May 2002

nj=5*round(2+x+4*x.^(1/3))+160;
e2=imag(m.*m);
dx=x/nj;
x2=x.*x;
nj1=nj+1;
xj=(0:dx:x);
en=Mie_Esquare(m,x,nj);
en1=0.5*en(nj1).*x2;   % End-Term correction in integral
enx=en*(xj.*xj)'-en1;   % Trapezoidal radial integration
inte=dx.*enx;
Qabs=4.*e2.*inte./x2;
result=Qabs;

4 Examples and Tests

4.1 The situation of x=1, m=5+0.4i

The execution of the command line
>> m =5 + 0.4i; x = 1; mie_abcd(m,x)

leads to column vectors $[a_n; b_n; c_n; d_n]$ for n=1 to n_{max}=7:

ans =

 Columns 1 through 4 (for n=1 to 4)

  0.2306 - 0.2511i   0.0055 - 0.0354i   0.0000 - 0.0008i   0.0000 - 0.0000i
  0.0627 + 0.1507i   0.0159 + 0.0262i   0.0004 - 0.0006i   0.0000 - 0.0000i
 -0.6837 + 0.0128i -0.3569 + 0.2199i   0.0752 + 0.0339i   0.0076 + 0.0000i
 -1.1264 + 0.0093i   0.2135 + 0.1212i   0.0180 + 0.0003i   0.0023 - 0.0004i

 Columns 5 through 7 (for n=5 to 7)

  0.0000 - 0.0000i   0.0000 - 0.0000i   0.0000 - 0.0000i
  0.0000 - 0.0000i   0.0000 - 0.0000i   0.0000 - 0.0000i
  0.0010 - 0.0002i   0.0002 - 0.0000i   0.0000 - 0.0000i
  0.0003 - 0.0001i   0.0001 - 0.0000i   0.0000 - 0.0000i

>> mie(m,x)

ans =

 Columns 1 through 7 (for m', m", x, Qext, Qsca, Qabs, Qb)

```
    5.0000    0.4000    1.0000    1.9794    0.8795    1.0999    1.1138
```

  Columns 8 through 9 (for <cosθ>, Qb/Qsca)

   -0.0595   1.2664

To test the absorption efficiency, call Mie_abs:

>> Mie_abs(m,x)

ans =

   1.0999

to confirm the result of mie(m,x), s. above.
Mie Efficiencies are plotted versus x (0≤x≤2) by Mie_xscan(m,201,0.01) in Fig. 1. Two absorption peaks can be observed near x=0.6 and 0.85 and a rapid variation of the scattering behaviour between the forward and backward hemisphere.
To plot the angular dependence of the scattered power in the two polarisations, the function Mie_tetascan(m,x,201), for x=1, is used to provide Figure 2.
Furthermore the absolute-square internal field is plotted versus the radial distance in Figure 3 by calling Mie_Esquare (automatically called by Mie_abs).
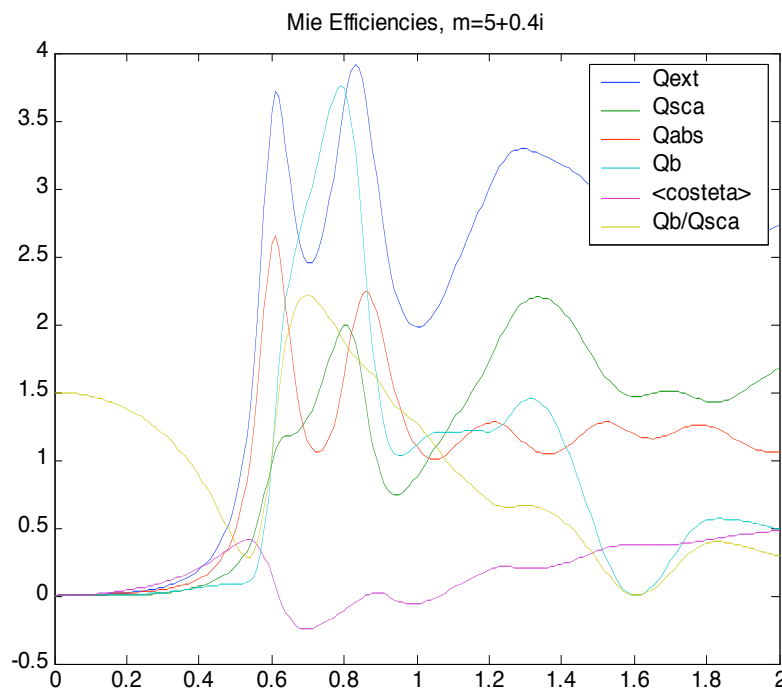

Figure 1: Mie Efficiencies for m=5+0.4i versus x, output of the function, Mie_xscan. Note the sign of <cosθ> changes a few times between x≅ 0.6 and 1.1.
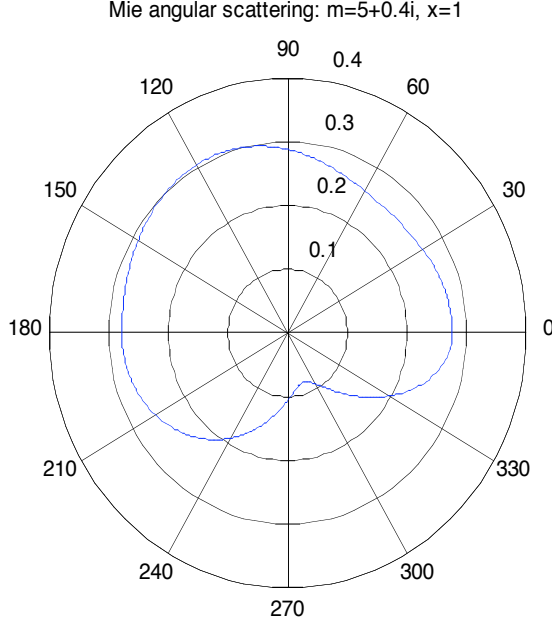
Mie angular scattering: m=5+0.4i, x=1

Figure 2: Angular Mie-scattering diagram of $|S_1|^2$ (upper Half circle) and of $|S_2|^2$ (lower half circle). Here, scattering in the backward hemisphere is slightly larger than in the forward hemisphere ($<\cos\theta>$ <0), a situation mostly restricted to the region near x=1.

Squared Amplitude E Field in a Sphere, m=5+0.4i, x=1

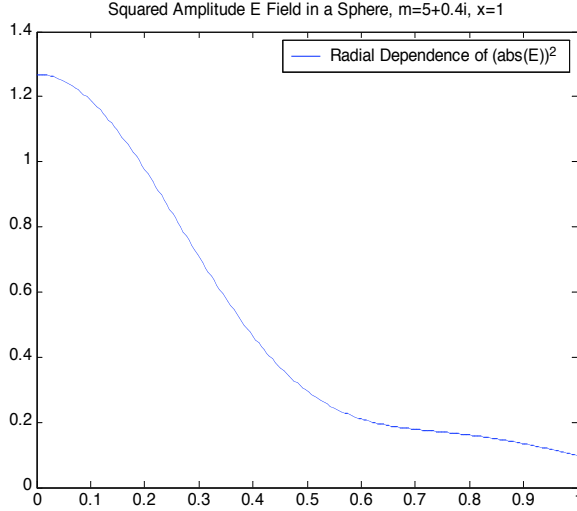Radial Dependence of (abs(E))²

Figure 3: Radial variation of the ratio of the internal/external absolute-square electric field with parameters given in the figure title. Here, the field is concentrated in the sphere centre.

To test the behaviour at low x values, Figure 1 indicates that the ratio Q_b/Q_{sca} approaches 1.5 near x=0. This is exactly the value obtained for Rayleigh scattering (Ishimaru, 1978). For x=0.1 Equation (9) gives absolute square internal field values between 0.0130 in the sphere centre and 0.0137 at the sphere surface, and for decreasing x the absolute square internal field of 0.0122 of the Rayleigh Expression (11) is reached at x=0.01. This means that the validity of the Rayleigh Approximation is quite limited, especially for large values of m.

4.2 Large size parameters

For x>>1, a large number of spherical harmonics have to be computed. Here we consider the example of m=2+0.01i. Figure 4 shows the Mie Efficiencies over the x range from 0 to 25. As a result of the Extinction Paradox (van de Hulst, 1957), Q_{ext} approaches the value 2 for very large x. The computed values are slightly higher in Figure 4. For increasing x, $Qext$ decreases to 2.09 at x=100, to 2.01 at x=2800 and to $Qext$=2.0014 for x=40'000. The program still works at x=70'000 ($Qext$ =2.0012), but for x>80'000 NaN values are returned.

In addition, for $x \gg 1$, the backscatter efficiency Q_b should approach the geometrical-optics expression

$$Q_b = \left| \frac{m-1}{m+1} \right|^2$$

which is 0.1111 in the present case. With $m=2+0.01i$, this value is obtained from the Function Mie for $x > 300$.
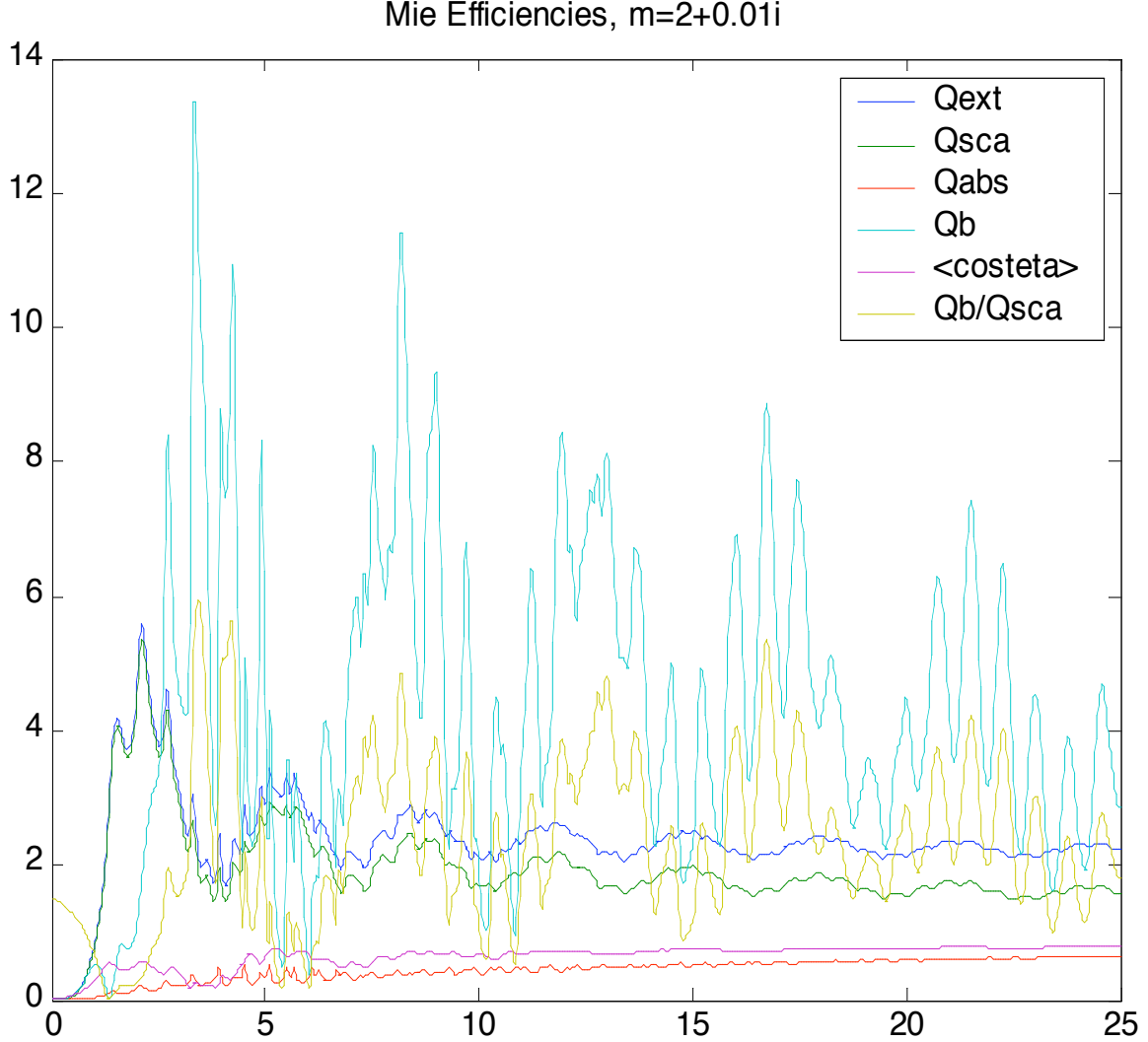

Figure 4: Mie Efficiencies for $m=2+0.01i$ over the x range from 0 to 25. The parameter with the maximum values and with the largest fluctuations is Q_b. The curves of Q_{ext} and Q_{sca} follow each other closely near values of 2. The lowest curve shows Q_{abs}, and $<\cos\theta>$ approaches 1 for high x values.

4.3 Large refractive index

Problems arise for high values of m. This situation occurs for metallic spheres, e.g. if $m=50+50i$, the maximum size parameter is about 13, and this value decreases with increasing m. A plot of efficiencies with $m=50+50i$ is shown in Figure 5, and the radial dependence of the absolute-square E field is shown in Figure 6 for $x=0.5$; the skin effect is very pronounced already at this small x value. Furthermore, due to

the acting depolarisation field, the internal field is very small even at the sphere surface.
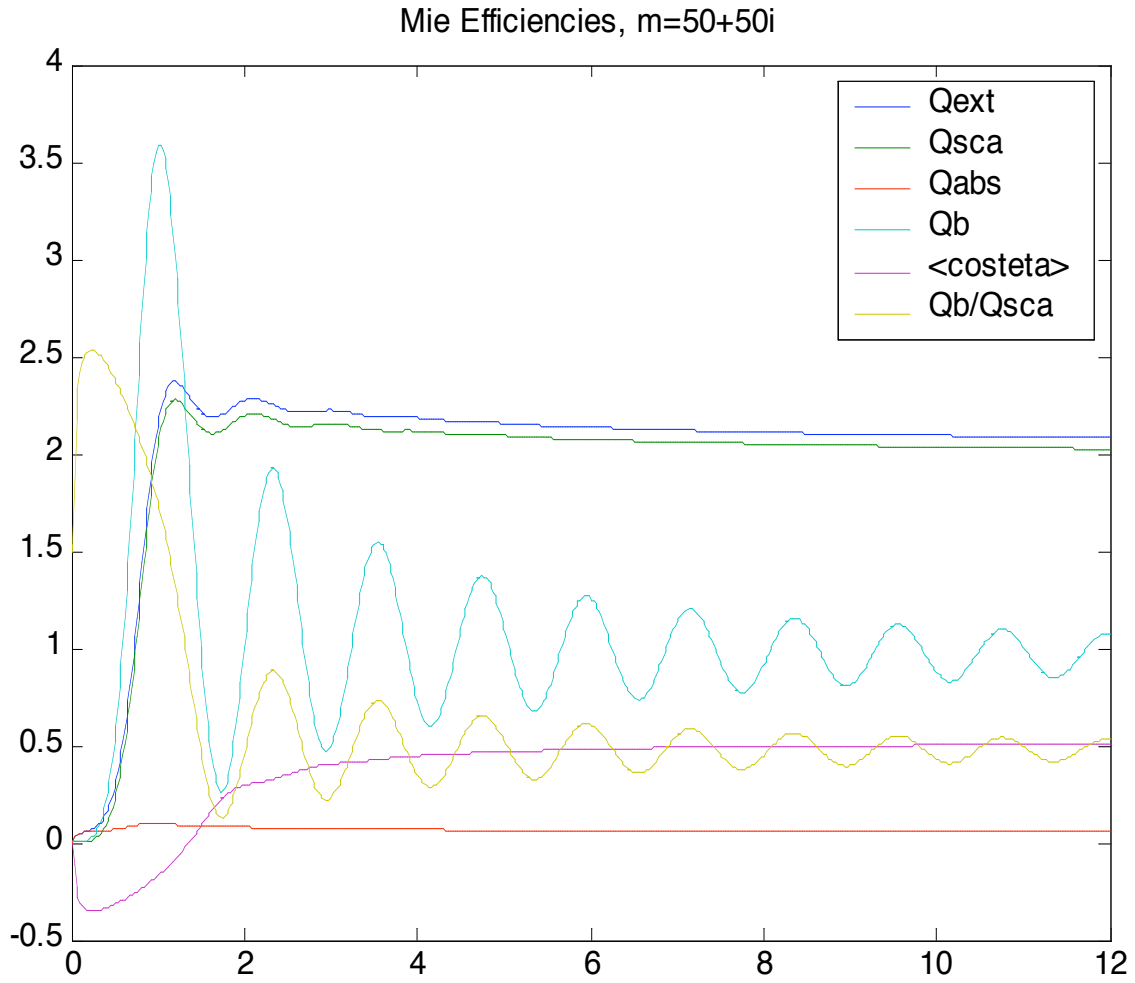

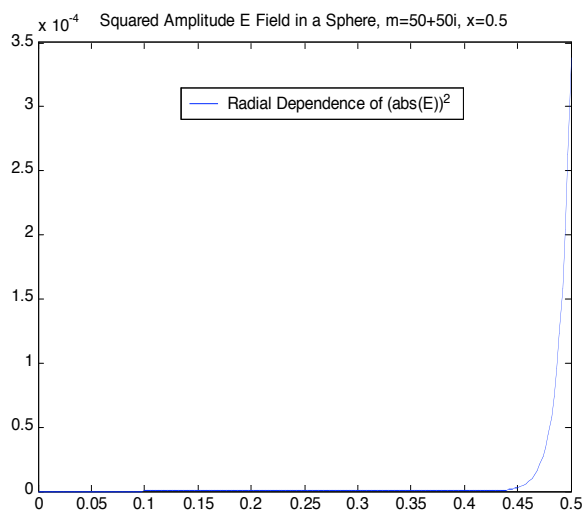Figure 5: Mie efficiencies for a metal-like material (m=50+50i).

Figure 6: Radial variation of the ratio of the internal/external absolute-square electric field for m=50+50i, x=0.5. The skin effect is clearly indicated by the concentration of the field near the sphere surface.

5 Conclusion, and outlook to further developments

The presented software represents the first major programming effort by the author in MATLAB; therefore the programs may not yet be optimum. Nevertheless, no severe problems have been encountered so far. Indeed, MATLAB appears to be a very efficient and accurate computing language suitable for the present application. However, further tests are required to get a more complete assessment of the Mie functions. Improvements are required to allow Mie computations for metal-like spheres over a larger x range than is presently possible.

Concerning further developments, the extension to situations with $\mu_1 \neq 1$ is straight-forward. Furthermore, it would be nice to make better use of the existing MATLAB visualisation tools. Finally, an extension to include scattering on coated spheres (BH, Section 8.1) and on other particles should be done as well.

References

Abramowitz M. and I.A. Stegun (eds.), "Handbook of Mathematical Functions", Dover Publication, New York, NY (1965).

Bohren C.F. and D.R. Huffman, "Absorption and Scattering of Light by Small Particles", John Wiley, New York, NY (1983).

Chandrasekhar S., "Radiative Transfer", Dover Publication (1960), BEWI TDD 211.

Deirmendjian, D. "Electromagnetic Scattering on Spherical Polydispersions", American Elsevier, New York, NY (1969).

Ishimaru A., "Wave propagation and scattering in random media", Vol. 1, Academic Press, Orlando, FL (1978).

Math Works, "MATLAB User's Guide", Natick, MA (1992).

Meador W.E. and W.R. Weaver, "Two-Stream Approximations to Radiative Transfer in Planetary Atmospheres: A Unified Description of Existing Methods and a New Improvement", J. Atm. Sciences, Vol. 37, pp. 630-643 (1980).

van de Hulst H.C. "Light Scattering by Small Particles", (1957), reprinted by Dover Publication, New York, NY (1981).